A Model Predictive Control with Non-Uniform Sampling Times for a Hybrid Energy Storage System in Electric Vehicle Application

João P. Trovão*, Maxime R. Dubois
e-TESC Laboratory / *INESC Coimbra
Department of Electrical & Computer Engineering
University of Sherbrooke
Sherbrooke, QC, J1K 2R1, Canada
{Joao.Trovao, Maxime.Dubois}@USherbrooke.ca

Oleg Gomozov[a], Xavier Kestelyn[a], Alain Bouscayrol[b]
[a] École Nationale Supérieure d'Arts et Métiers, L2EP
[b] University of Lille1, L2EP
59000 Lille, France;
{Oleg.Gomozov, Xavier.Kestelyn}@ensam.eu
Alain.Bouscayrol@univ-lille1.fr

***Abstract*—In this paper, the simulation of a semi-active hybrid topology for urban electric vehicle is developed in order to define an effective energy management system. The overall powertrain model including its inner control layer is fully addressed using energetic macroscopic representation to introduce the energy strategy level. This management strategy is supported by model predictive control using non-uniform sampling time concept. Simulation with Matlab-Simulink™ are provided to demonstrate the performance of the selected topology when tailored by a strategy that maintaining within physical and accurate limits the batteries and supercapacitors currents, and batteries and supercapacitors state-of-charge on the driving cycle.**

***Keywords*—Urban Electric Vehicles, Energy Management Strategy, Model Predictive Control, Supercapacitors, Batteries, Non-Uniform Sampling Times.**

I. INTRODUCTION

Environmentally friendly commercial vehicles such as battery-only Electric Vehicles (EVs) are increasingly studied and manufactured at present to minimize environmental impacts [1, 2]. Specifically, in this days, EVs have extensively developed for urban purposes, ensuring better performance in terms of maneuverability, dynamic capability and lethality. For achievement of these requirements, urban EVs require features such as high climbing and fast acceleration capabilities, and energetic efficiency. Therefore, various hybrid topologies of energy storage system, including batteries and supercapacitors (SCs), should be appropriately combined considering the performance requirements, energy economy, as well as driving cycle completeness [3]. The main idea is supported by the use in the same energy storage system of high specific energy (energy battery) and high specific power (SCs) storage elements. The topology that offers the highest level of freedom is the fully-decoupled [4]-[6]. For the cost point of view, automotive industry has been more interested by solution with less power components requests, and semi-decoupled topology draw some new perspectives [7]. The use of only a DC-DC converter is more attractive, but the demand of a quasi-constant DC Bus and improved strategy to share the power between the two energy storage element still a challenge. The primary request is related to the overall efficiency of the traction system in order to reduce the drive and motor losses and temperature [4]. The second is linked to the effective usage of the SCs, given their complementarity to the energy battery pack [7]. In urban driving cycle where a high number of stop-and-go operations occur, the SCs characteristics is fundamental to reduce the stresses in batteries current and increase the life cycle of this primary energy sources in EVs [8].

The aim of this paper is to extend the previous work [9, 10] based on energy management system (EMS) for fully-decoupled topology to a simpler and reduced cost configuration: semi-decoupled hybrid topology. The EVs using batteries and SCs is studied, developing a functional model supported by Energetic Macroscopic Representation (EMR). The inner control layer is deduced based on the maximum control structure using the inversion-rules of EMR approach. Thereafter, the EMS is developed on the first control layer in order to take into consideration the system dynamics, addressing the two fundamentals problems of the vehicle management: energy and power. The requirement to control an energy storage system with two different storage systems and only one DC-DC converter leads to the use of an improved EMS and Model Predictive Control (MPC) fulfill these requirements [11]. The proposed approach considers the diverse specifications of the system using a set of constrains and includes some king of future power demand prediction. The final part of this paper introduce the development of an energy strategy based on a MPC with non-uniform sampling times.

The remainder of this paper is organized as follows. Section II depicts a description of the powertrain system. Section III is devoted to the EMR modelling and inner control layer development. Section IV focuses on the MPC with non-uniform sampling times applied to EMS definition. Section V provides the simulation results. In the final section, some conclusions and final remarks are draw.

II. POWERTRAIN SYSTEM

The studied topology is aimed to be implemented on an urban small dimension EV, based on a second generation of a SMART vehicle (see Fig. 1), and converted into electric propulsion vehicle by ATEUS (*Association des Transports*

978-1-4673-7637-2/15/$31.00 ©2015 IEEE

Électriques de l'Université de Sherbrooke) under e-VUE project. The original version of this EV is powered using a Li-ion battery pack (7.68 kWh) and propelled by a rear-mounted Permanent Magnet Synchronous Motor (PMSM) of 30 kW, 5500 rpm.

Fig. 1. ATEUS electric vehicle prototype

Table I presents the principal characteristics of the ATEUS prototype.

TABLE I. ELECTRIC VEHICLE SPECIFICATIONS

Variable	Symbol	Value	Units
Vehicle mass (without battery and SCs packs)	m	795	kg
Rolling resistance force	μ_{rr}	0.02	-
Gravity acceleration	g	9.81	m/s^2
Air density @ 20ºC	ρ	1.223	kg.m^{-3}
Aerodynamic drag coefficient (with driver)	C_D	0.35	-
Vehicle front area	A_f	2.4	m^2
Wheels radius	r	0.38	m
Gearbox transmission ratio	G_{gb}	3 (3:1)	-
Gearbox transmission efficiency	η_{gb}	92	%

The semi-active topology to couple a SCs pack is proposed to increase the dynamic performance of the EV prototype. The SCs pack is connected to the common DC Bus that connects the battery pack to the motor drive. A DC-DC converter is used to control the current flow of the SCs to or from the DC Bus. This topology is under study to improve the first version of the e-VUE prototype. Some challenges are related to the inner control layer of this topology, namely, the diminution of hard DC Bus voltage fluctuations in order to reduce the motor and drive losses [4]. When the battery pack is directly coupled to the motor inverter the voltage variation is directly linked to the battery current discharge. With the addition of the second energy storage element with a DC-DC converter, the inner control layer and the EMS have, as a first objective, to stabilize the voltage at the inverter terminals. The proposed powertrain architecture is presented in Fig. 2.

For the proposed study, the battery pack is characterized by LiFePO4 cells, 3.2 V and 14.5 A@1C. The SCs pack based on a 250 F module (16.2 V) is used to reduces the current stress in the batteries and improve the EV dynamics. Table II present the main characteristics used to model the energy storage system.

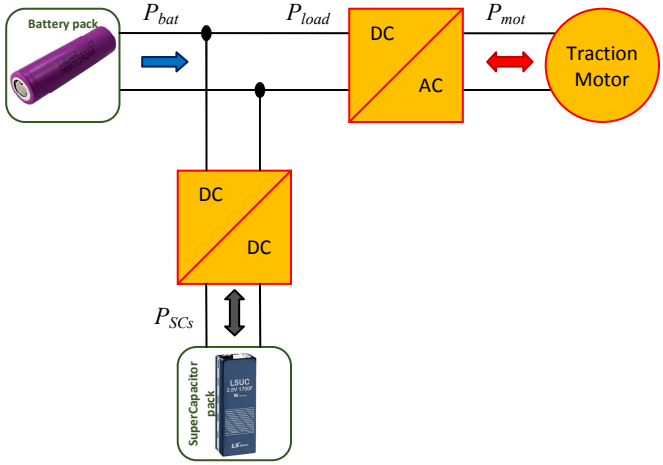

Fig. 2. Power train architecture

TABLE II. CHARACTERISTICS OF THE ENERGY STORAGE SYSTEM

Variable	Symbol	Value	Units
Battery (3.2 V EiG LiFePO4 cell)			
Battery pack Power	P_{Bat}	[- 1.2, 9.5]	kW
Battery pack SoC Limits	SoC_{Bat}	[0.2, 1]	-
Min. cell open-circuit voltage	$V_{Bat}^{OC\_min}$	2.4	V
Cell no-load voltage drop	δ_{bat}	1.0	V
Max. cell open-circuit voltage	$V_{bat}^{OC\_max}$	3.4	V
Cell internal resistance	R_{cell}	5	mΩ
Number of batteries in series	N_{cell}	96	-
Num. of battery's bank in parallel	n_{cell}	2	-
Battery mass	M_{cell}	0.4	kg
Supercapacitors (MAXWELL BMOD0250 modules)			
SC module Capacitance	Cap_{SCs}	250	F
SC pack Power	P_{SCs}	[- 96, 96]	kW
SC pack SoC Limits	SoC_{SCs}	[0.5, 1]	-
Min. SC open-circuit voltage	$V_{SCs}^{OC\_min}$	0	V
SC no-load voltage drop	δ_{SCs}	16.2	V
SC pack operation range	V_{SCs}^{OC}	[64.8, 129.6]	V
SCs module internal resistance	R_{SCs}	4.1	mΩ
Number of SC's module in series	N_{SCs}	8	-
Num. of SC's module in parallel	n_{SCs}	2	-
SC Mass	M_{SCs}	4.45	kg

III. EMR MODELLING APPROACH

EMR is a graphical description that highlights the energy properties of components within a system in order to develop control schemes [9, 10] (see Appendix for the pictograms). Only the physical causality (i.e. integral causality) is considered. Moreover, all elements are connected according to the interaction principle: the product of the action and the reaction variables yields the power exchanged. The overall EMR model is presented in Fig. 3, including all the mechanical and electrical components models.

A. Energy Storage Elements

Batteries and SC are the energy sources (green oval pictograms). In the EMR approach, the source imposes the voltage $v_j(t)$ in the system, which responds with the current $i_j(t)$ ($j \in \{Bat; SC_s\}$). For energy analysis, a simple energetic model could be used, as presented in (1).

$$v_j(t) = \left[V_j^{OC\_min} + \delta_j \cdot SoC_j(t)\right] - R_j \cdot i_j(t) \qquad (1)$$

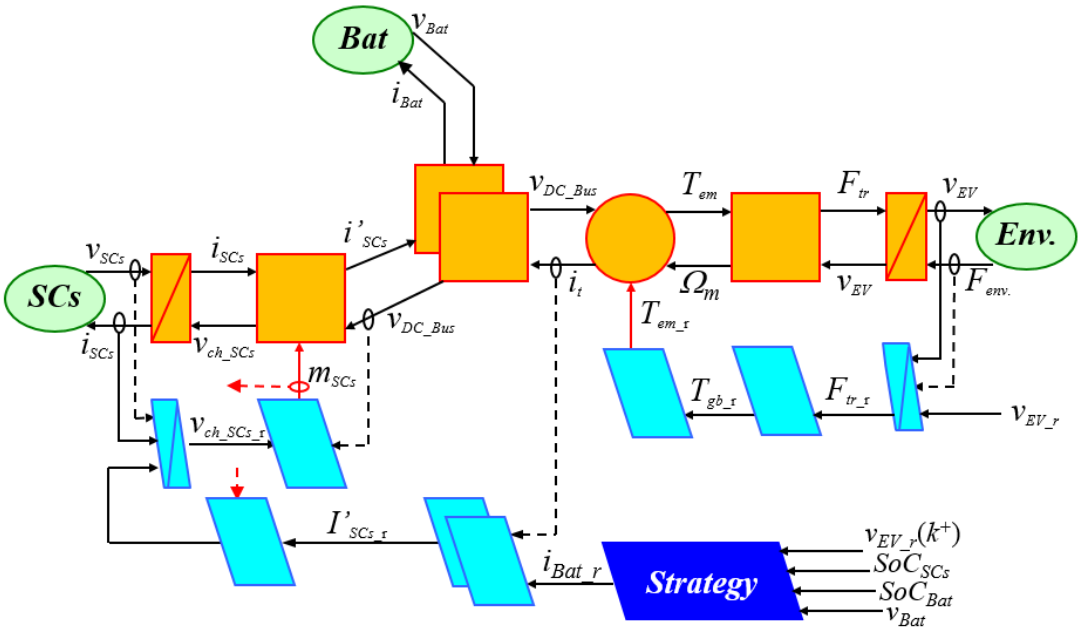

Fig. 3. EMR and maximum control structure for the studied EV

where the State-of-Charge (SoC_j) and the charge evolution Q_j are linked by:

$$SoC_j(t) = \frac{Q_j(t-\Delta t) - \int_0^{\Delta t} i_j(t)\cdot dt}{Q_j^{ref}} \tag{2}$$

with $V_j^{OC\_min}$ is the minimum open-circuit voltage; δ_j is the no-load voltage drop; and R_j is the internal resistance of the energy storage element.

B. DC-DC Converter

The inductor is modelled as an accumulation element (orange crossed rectangle) that impose the current as a state variable (output) from different input voltages (3). L_{SCs} and $R_{L_{SCs}}$ are the inductance and resistance of the this inductor.

$$L_{SCs}\cdot\frac{di_{SCs}}{dt} = v_{SCs} - v_{ch\_SCs} - R_{L_{SCs}}\cdot i_{SCs} \tag{3}$$

The DC/DC converter is a mono-physical conversion element (orange square). This device is typified using a modulation ratio m_{SCs} that connect the voltages and currents from both sides (4), where η_{Conv} is the DC-DC converter efficiency.

$$\begin{cases} v_{ch\_SCs} = m_{SCs}\cdot v_{DC\_Bus} \\ i'_{SCs} = m_{SCs}\cdot i_{SCs}\cdot \eta_{Conv}^{\beta} \end{cases}$$
$$m_{SCs}\in\{0,1\} \text{ and } \begin{cases} \beta = 1, \text{for } P_{Conv}\geq 0 \\ \beta = -1, \text{for } P_{Conv} < 0 \end{cases} \tag{4}$$

C. DC Bus

The common DC Bus couples the batteries, the SCs DC-DC converter and the traction system (inverter and motor). The common voltage $v_{DC_{Bus}}$ is represented by a distribution element (orange double square), with the following currents and voltages relations:

$$\begin{cases} i_{Bat} = i_t - i'_{SCs} \\ V_{DC_{Bus}} = V_{Bat} \end{cases} \tag{5}$$

D. Motor, Inverter and Mechanical Transmission System

The global model of the traction system was developed using a generic model of the electric machine and its inverter. To study the energy management problem, a static model is used [10]. This model takes into account the inverter, PMSM and its control for a low fluctuation DC Bus voltage and nominal temperature. The PMSM is directly controlled by a reference torque and the current is modeled by:

$$\begin{cases} T_{em} = T_{em\_r} \\ i_{load} = \frac{T_{em}\Omega_m\eta_m^{\beta}}{v_{DC}} \end{cases} \begin{cases} \beta = 1, \text{for } T_{em}\geq 0 \\ \beta = -1, \text{for } T_{em} < 0 \end{cases} \tag{6}$$

where η_m is the efficiency of the PMSM as a function of the torque and speed variation, as presented in Fig. 4.

The PMSM torque T_{em} is applied directly on the gearbox and the traction wheels, resulting in the rotor rotation speed Ω_m and the traction force F_{tr}. The used EMR approach uses an integrated model for the gearbox and wheels, represented by a mono-physical conversion element (orange square).

$$\begin{cases} F_{tr} = \frac{G_{gb}}{r}T_{em}\eta_{gb}^{\beta} \\ \Omega_m = \frac{G_{gb}}{r}v_{EV} \end{cases}, \begin{cases} \beta = 1, \text{for } P_{mec}\geq 0 \\ \beta = -1, \text{for } P_{mec} < 0 \end{cases} \tag{7}$$

where G_{gb} is the fixed gear ratio, η_{gb} its efficiency, and r the wheel radius. The slip phenomenon of the wheels is disregarded and all inertias are mixed with the vehicle mass.

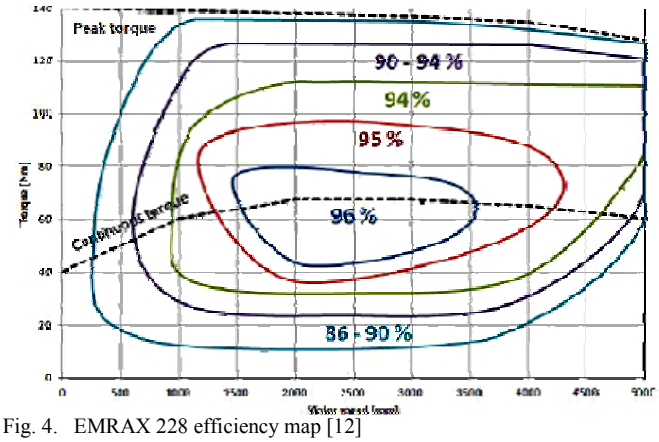

Fig. 4. EMRAX 228 efficiency map [12]

The kinetic energy accumulation on the chassis is modeled by an accumulation element (orange crossed rectangle), obtening the vehicle speed v_{EV} as the state variable of this accumulation element, derived from the total traction force F_{tr} and the traction force resistance, F_{env}:

$$M_{eq}\frac{d}{dt}v_{EV} = F_{tr} - F_{env} \tag{8}$$

where M_{eq} is the equivalent mass of the vehicle, considering the tare weight, energy sources, passengers and minor inertia effects (wheels, shafts, etc.).

Finally, the action of the environment on the vehicle is modeled as a mechanical source yields the traction force resistance F_{env} mainly composed of drag, friction and slope components, as presented in (9).

$$F_{env} = \mu_{rr}\, M_{eq}\, g + \frac{1}{2}\rho\, A_f\, C_d v_{EV}^2 + M_{eq}\, g\, sin(\theta) \tag{9}$$

E. Inner Control layer

Using the EMR of the studied powertrain system, the control scheme can be directly deduced from the inversion of the EMR blocs [7, 9, 10], as presented in Fig. 3.

The primary objective is that the EV prototype follows the vehicle reference (standard driving cycle). For this a reference for the PMSM torque should be computed as a function of the vehicle speed v_{EV}. The vehicle speed, v_{EV}, is compared to the imposed speed reference in order to determine the traction force reference as presented in (10), using a speed controller $C_S(t)$.

$$F_{tr\_r} = \left(v_{EV_r} - v_{EV}\right)C_S(t) + F_{env} \tag{10}$$

Thereafter, the reference torque to apply on the PMSM, T_{em_r}, is derived from the inversion of (6) given (11):

$$T_{em\_r} = \frac{r}{G_{gb}}F_{tr\_r} \tag{11}$$

The second objective is the control of the SCs current. For that, the tuning variables m_{SCs} to operate the DC-DC converter in order to indirectly perform a short variation on the $v_{DC_{Bus}}$, using the causality principle. The SCs inductor current is the state variable in this control loop. Then, a current controller is required to invert (3) and to define the reference voltage $v_{ch\_SCs\_r}$ from i_{SCs_r} exploiting the SCs voltage (v_{SCs}) as compensation for the current controller, $C_{I_{SCs}}(t)$, defined by (12):

$$v_{ch\_SCs\_r} = v_{SCs} - \left(i_{SCs\_r} - i_{SCs}\right)C_{I_{SCs}}(t) \tag{12}$$

For (12), the SCs current reference, i_{SCs_r}, is deduced using the contribution of the battery to the total traction system current (i_t), and reduced to the low side of the DC-DC converter:

$$i_{SCs\_r} = \frac{v_{DC\_Bus}}{v_{SCs}} \cdot \left(i_t - i_{Bat_r}\right) \tag{13}$$

The reference of battery pack current, i_{Bat_r}, is given by upper control layer, that defines the energy strategy options implemented at the vehicle EMS.

IV. Energy Management System

The fundamental objective of the developed EMS is never overloading the battery pack while keeping the DC Bus voltage into a close range near to its nominal value. For this, the used strategy should be regulate the available energy in the SCs (SCs SoC) in order to assist the batteries in the feeding process of the power demand. An effective management of the energy and power is required based on a long-term planning. For that purpose, the MPC is in charge of the long term horizon forecast and in order to regulate the SCs SoC to be fully prepared to help the energy storage system to have faster dynamics and reduce the stress on the batteries.

At a higher level, the decision about the charging or discharging the SCs should be taken to regulate the energy level to an accurate level for the next operation power requests. To give the SCs current reference in addition to the global current, a fast alternating directions method of multipliers (ADMM) based MPC supervisor is developed to solve the optimization problem depicted in the following [13]-[15]:

Minimize:

$$\sum_k \begin{pmatrix} \omega_1^k (P_t - P_{Bat} - P_{SCs})^2 \\ +\omega_2^k (\Delta P_{Bat})^2 \\ +\omega_3^k \left(SoC_{SCs} - SoC_{SCs}^{ref}\right)^2 \\ +\omega_4^k \left(SoC_{Bat} - SoC_{SCs}^{ref}\right)^2 \end{pmatrix} \tag{14}$$

Subject to:

$$SoC_{Bat}(k+1) = SoC_{Bat}(k) - \frac{P_{Bat}(t)\cdot \Delta T(k)}{E_{Bat}^{max}} \tag{15}$$

$$SoC_{SCs}(k+1) = SoC_{SCs}(k) - \frac{P_{SCs}(t)\cdot \Delta T(k)}{E_{SCs}^{max}} \tag{16}$$

$$SoC_{SCs}^{min} \le SoC_{SCs}(k) \le SoC_{SCs}^{max} \tag{17}$$

$$SoC_{Bat}^{min} \le SoC_{Bat}(k) \le SoC_{Bat}^{max} \tag{18}$$

$$P_{SCs}^{min} \le P_{SCs}(k) \le P_{SCs}^{max} \tag{19}$$

$$P_{Bat}^{min} \leq P_{Bat}(k) \leq P_{Bat}^{max} \quad (20)$$

Non-uniformly distributed sampling time over prediction horizon is used to couple the short and long term predictions for allowing better required energy reserve estimation.

In the implemented MPC algorithm, the approach is linear with non-uniformly distributed sampling time and use a box constraints on inputs and outputs of the system (15)-(20). The limits of the SoC_{SCs} are set to 95% (for its maximum) and 50% (for its minimum). Regarding the sampling time (ST), we used a distribution based on:

$$ST = ST^{min} + \frac{(ST^{max} - ST^{min})}{1 + e^{-index/10}} \quad (21)$$

with ST^{min} set to 0.3 s, ST^{max} set to 20 s, and $index$ is a vector of integers. The total prediction horizon is 20 samplings.

The proposed approach allows the coupling between fast dynamics of the SCs and batteries, SoC management and energy flows optimization. The optimization problem is solved by interior point method iteratively and allows real-time evaluation on intel core i7 1.7 GHz processor.

The energy management approach is established with long- and short-term decision and coupled to the inner control loop.

V. First Simulation Results

The simulation is developed on a Matlab/Simulink™ environment, using a PI controller for the current and EV speed controller. The driving cycle used for this test was VWU-CITY, using as reference the double of the normalized speed. The initial SCs SoC was set to 90%. The battery and SCs measured currents following the currents and the EV speed reach the suggested dynamics by the standard driving cycle references, as presented in Fig. 5. The results show the reliability of the controllers.

Analyzing the power demands at the batteries and SCs, a large part of the higher frequencies of the power demand were transferred to the SCs pack and the batteries never feed more than its nominal power at 1C. These results demonstrate that the strategy and decision taking at the EMS level is well tuned and accurate for the urban driving profile.

VI. Conclusions

A model based on EMR approach of an EV was developed and fully simulated using EMR approach. The presented simulations results validate the inner control layer and the proposed energy management strategy based on an original configuration of MPC with non-uniform sampling times. Using a specific case study of semi-decoupled hybrid topology to combine batteries and SCs in EV application, the proposed scheme could be evaluated to show its effectiveness in reducing the stress on the battery pack (hence its temperature) and the overall powertrain efficiency, as well as the applicability of MPC with non-uniform sampling times to fast dynamics problems.

This procedure is inserted into a more global approach in order to accelerate testing and validation time. The following steps will be based on extend the study with a reduced-scale prototype in a laboratory controlled environment before real-scale prototype implementation.

Appendix

Table III shows a summary of the EMR.

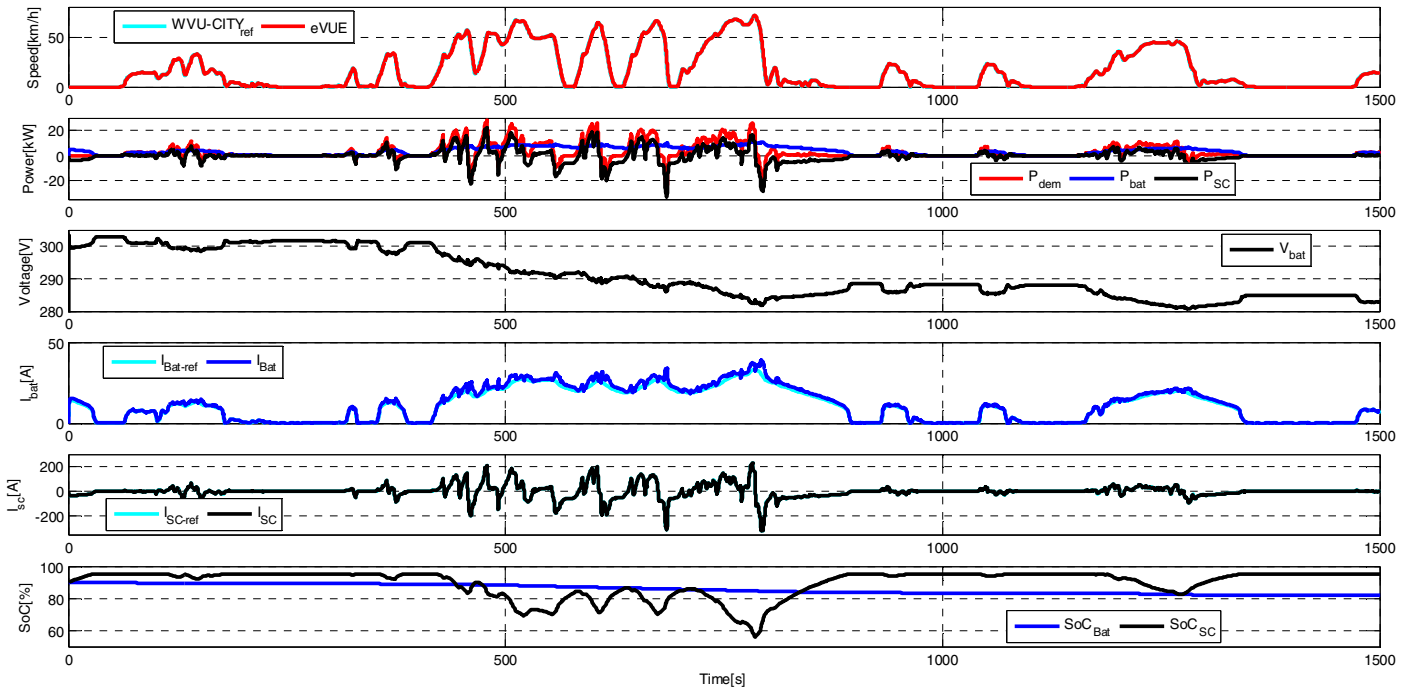

Fig. 5. Simulation results of the e-VUE prototype using a semi-decoupled hybrid topology with a SCs pack.

TABLE III. SUMMARY OF ENERGETIC MACROSCOPIC REPRESENTATION PICTOGRAMS

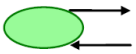	Source element (energy source)	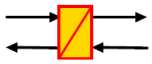	Accumulation element (energy storage)	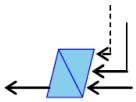	Indirect inversion (closed-loop control)
		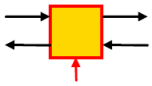	Mono-physical conversion element		Direct inversion (open-loop control)
 Sensor Mandatory Optional		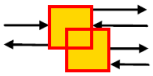	Mono-physical coupling element (energy distribution)	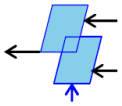	Coupling inversion (energy criteria)

ACKNOWLEDGMENT

This work was supported in part by the *Programme Samuel-De Champlain de la 65e session de la Commission permanente de coopération franco-québécoise* and by Natural Sciences and Engineering Research Council of Canada.

REFERENCES

[1] C.C. Chan, The state of the art of electric, hybrid, and fuel cell vehicles, Proc. of the IEEE, vol. 95, n.4, pp. 704 – 718, April 2007.

[2] R. Barrero, J. Van Mierlo, X. Tackoen, Energy savings in public transport, IEEE Veh. Tec. Magazine, vol. 3, n. 3, pp. 26-36, Sep. 2008.

[3] A. Khaligh, Zhihao Li, Battery, Ultracapacitor, Fuel Cell, and Hybrid Energy Storage Systems for Electric, Hybrid Electric, Fuel Cell, and Plug-In Hybrid Electric Vehicles: State of the Art, IEEE Trans. Veh. Tec., vol.59, n.6, pp. 2806-2814, Jul. 2010.

[4] Trovão, J.P.; Pereirinha, P.G., "Control scheme for hybridised electric vehicles with an online power follower management strategy," Electrical Systems in Transportation, IET , vol.5, no.1, pp.12-23, 3 2015

[5] T. Azib, O. Bethoux, G. Remy, C. Marchand, Saturation Management of a Controlled Fuel-Cell/Ultracapacitor Hybrid Vehicle, IEEE Trans. Veh. Tec., Vol. 60, n. 9, pp. 4127-4138, Nov. 2011.

[6] Jian Cao, A. Emadi, A New Battery/UltraCapacitor Hybrid Energy Storage System for Electric, Hybrid, and Plug-In Hybrid Electric Vehicles, IEEE Trans. Power Electr., vol. 27, n. 1, pp. 122-132 Jan. 2012.

[7] Castaings, A.; Lhomme, W.; Trigui, R.; Bouscayrol, A., "Different Control Schemes of a Battery/Supercapacitor System in Electric Vehicle," IEEE Vehicle Power and Propulsion Conference (VPPC 2014), pp. 1-6, 27-30 Oct. 2014.

[8] Trovao, J. P.; Santos, V.; Antunes, C. H.; Pereirinha, P.; Jorge, H., "A Real-Time Energy Management Architecture for Multi-Source Electric Vehicles," IEEE Transactions on Industrial Electronics, vol. 62, n. 5, May 2015.

[9] A.-L. Allegre, A. Bouscayrol, R. Trigui, Flexible real-time control of a hybrid energy storage system for electric vehicles, Electrical Systems in Transportation, IET, vol.3, n.3, pp.79-85, Sep. 2013.

[10] J. P. Trovão, A. Bouscayrol, F. Machado, W. Lhomme, "Hierarchical Management Structure of a Battery Supercapacitor System for EV Using Energetic Macroscopic Representation", 11th International Conference on Modeling and Simulation of Electric Machines, Converters and Systems, ElectrIMACS 2014, Valence, Spain, May 19-22, 2014.

[11] Pant, Y.V.; Nghiem, T.X.; Mangharam, R., "Peak power reduction in hybrid energy systems with limited load forecasts," American Control Conference (ACC), pp.4212,4217, June 2014

[12] ENSTROJ, electric motor innovation, "Manual for EMRAX motors", Dez. 2014, available at http://www.enstroj.si/

[13] O'Donoghue, B.; Stathopoulos, G.; Boyd, S., "A splitting method for optimal control", IEEE Trans. Cont. Sys. Tech., vol.21, n.6, pp. 2432-2442, Jul.2013.

[14] Goldstein, T.; O'Donoghue, B.; Setzep, S.; Baraniuk, R., "Fast alternating direction optimization methods", SIAM Journal on Image Sciences, vol.7, n.3, pp.1588-1623, Aug. 2014.

[15] Ghadimi, E.; Teixeira, A.; Shames, I.; Johansson, M., "Optimal parameter selection for the Alternating Direction Method of Multipliers (ADMM): Quadratic problems", IEEE Trans. Aut. Cont., vol.60, n.3, pp.644-658, March 2015